Properties of Sharav (Khamsin) Dust—Comparison of Optical and Direct Sampling Data

ZEV LEVIN, JOACHIM H. JOSEPH AND YURI MEKLER

Department of Geophysics and Planetary Sciences, Tel Aviv University, Ramat Aviv, Israel

(Manuscript received 27 August 1979, in final form 3 December 1979)

ABSTRACT

Simultaneous measurements of optical depth and size distribution in a dust storm are presented. The measured and derived properties of the aerosol are compared with each other and with other results published in the scientific literature. We observe some global commonality in the measured size spectra of desert aerosols especially for post-frontal conditions. On the other hand, during the passage of the front itself, high aerosol concentrations with a sharp peak in radius at ~ 1 μm were observed. Generally, these were not similar to other size distributions reported in the literature.

The imaginary part of the refractive index in the spectral region 0.3–1.7 μm was found to be similar to that found in other deserts. Comparison of the optical measurements with the direct sampling data suggests that the general time trends of the size distributions, as measured *in situ*, are followed by the optical depth and its variations with wavelength. On the other hand, detailed short-term fluctuations detected by our direct measurements are not followed by the optical method. We have observed that a simple power law for the size distribution, in the range $r > 0.15$ μm, is a reasonable approximation only during clear and calm conditions with small optical depth. During the dust storm itself, the deviations from a power law are large as shown by both direct *in situ* and optical observations.

1. Introduction

Wind-blown dust is one of the major sources or components of natural and man-made aerosols in the atmosphere (e.g., SMIC, 1971; Carlson and Prospero, 1972; Carlson, 1976). Desert dust is in turn an important part of dust aerosol and of the so-called "background aerosol"; its source regions cover one-third of the world's land surfaces and its sinks are global (Goldberg, 1971).

There is much intrinsic interest in the investigation of the physical and chemical properties of the desert aerosol with a view to evaluating the latter's potential direct and indirect climatic effects (e.g., Joseph *et al.*, 1973, Joseph and Wolfson, 1975; Joseph, 1976; Carlson and Prospero, 1972; De Luisi *et al.*, 1976a,b).

Most experimental studies of the desert aerosol, or of any aerosol, suffer from the fact that it is fairly difficult to study a pure mono-source natural aerosol without admixtures of other aerosols, clouds or gases. This paper concentrates on a case study in which it was possible to isolate clearly one single aerosol type. We carried out simultaneous *in situ* measurements of aerosol size distributions of the imaginary part of the refractive index as well as of spectral transmission of the atmosphere to solar radiation. The simultaneous time histories of some of these quantities will be presented and intercompared in this paper. Furthermore, the results will be compared with relevant data in the literature.

A severe Sharav (Khamsin) dust storm occurred on 6 June 1977, brought on by the passage of a thermal low-pressure system coming from the North Africa deserts over Israel (see Figs. 1a and 1b). The cold front seen in the figure passed the observing site at about 1200 LST. Winds were mostly from the south-southwest before the frontal passage and did not exceed 5 m s^{-1} at our station. After the front passed, the wind shifted to more westerly flow with speeds of up to 10 m s^{-1}. No clouds were observed during the major part of the storm and the relative humidity decreased continuously from the morning (51% at 0800 LST) to evening hours (17% at 2000 LST). The observed optical depths were larger than 1.0 and reached values larger than 3.0, thus making the aerosol by far the dominant absorber and scatterer of solar radiation.

The dust first appeared at higher altitudes before it was detected at the surface. This resulted in a milky white sky overhead, while the horizontal visibility remained at 40–50 km from the morning hours until about 1100, when it decreased and varied between values of 1 to 10 km. The source of the dust brought to the region of our observations by long-range atmospheric transport is the North African Desert (mostly Libya and Egypt).

0022-4928/80/040882-10$06.50

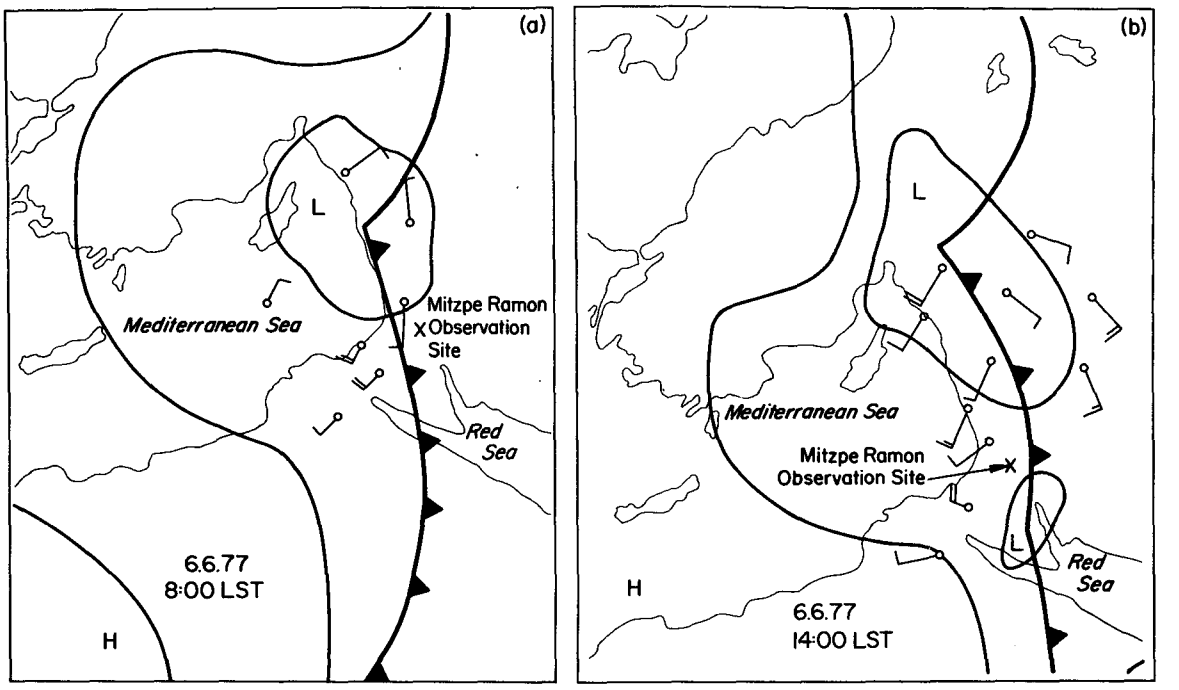

FIG. 1. Synoptic maps of the weather situation on 6 June 1977 at 0800 and 1400 LST.

2. The data acquisition systems

The experimental systems were set up at the Wise Astronomical Observatory of Tel Aviv University near Mitzpe Ramon in the High Negev Desert (30.596°N, 34.762°E at 890 m MSL). Aerosol size distributions were measured automatically every 15 min during the day and night with a well-calibrated Royco optical counter (Model 220) (see Levin and Lindberg, 1979) placed on the roof top of the observatory (5 m above ground). The instrument classifies particles into six size intervals (0.15–0.32, 0.32–0.75, 0.75–1.50, 1.50–3.00, 3.00–7.5 μm and particles > 7.5 μm radius) and its output is recorded on punched paper tape.

The aerosols were also collected on millipore filters (0.45 μm pore size) for later analysis of the imaginary part of the refractive index as a function of wavelength in the visible. Due to the need for relatively large amounts of dust for this analysis, the sample was collected over a 14-day period which included the Sharav day. The optical analysis of the samples was carried out by the Kubelka-Munk reflection spectroscopy technique (Lindberg, 1975) at the U.S. Army laboratories at White Sands.

Solar radiation measurements were taken with a six-channel sun-following automatic spectro-radiometer equipped with six interference filters of 0.01 μm half-width (see Fig. 2). The solar radiation is collimated to provide an effective field of view of 1°. The instrument is calibrated by use of both laboratory techniques and by a Langley plot (e.g., King *et al.*, 1978).

Measurements of surface temperature and humidity as well as pressure and wind were available. Radiosonde data were also available from Beit Dagan (~170 km away).

3. Data and Analysis

a. Size distribution

Surface measurements of the aerosol size distributions suggest that large changes occur in the latter during the passage of the front. The curves with open circles in Fig. 3 present the mean total number concentrations (mean of four measurements every 15 min) as a function of time as determined by the Royco counter. We clearly see the sharp increase in aerosol concentration during the passage of the cold front (see Fig. 3). The atmospheric aerosol load began to increase even before 1000 (about 1.5 h ahead of the front), and decreased sharply over a few hours following the frontal passage. The change of aerosol concentration with time is similarly shown in Fig. 4, which presents detailed size distributions $dN/d\log r$ vs $\log r$). One can see that the peak of the size distribution around 1 μm becomes very prominent around the time of the passage of the front and disappears gradually afterward. The average slope of the distribution between 2 and 10 μm radius remains approximately constant for over a day at a value of ~2.3. Only two

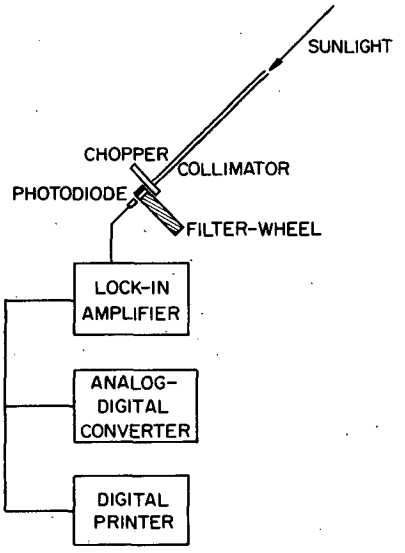

FIG. 2. The normal-incidence sun-following automatic interference filter spectrophotometer.

days later does the slope approach that of a typical distribution for the region (marked average winter day on Fig. 4). A closer look reveals that at 1000 LST 6 June (prior to the passage of the cold front), a flat-top distribution (over the range 0.15–1.5 μm radius) had developed as a result of the increase in the number concentration of particles ~1–1.5 μm in radius. This increase is further emphasized at 1130, just prior to the passage of the front when a maximum ~1–1.5 μm had developed. One should also note the slight increase in the number concentration of the largest particles (~10 μm) which suggests the presence of a second peak at larger sizes, not resolved by our instrument.

Comparison of our data, after the peak of the Sharav (e.g., 1500 LST onward), with the aerosol size distribution measurements at Haswell, Colorado as reported by Patterson and Gillette (1977, hereafter designated PG) shows the similarity of the distributions at the two locations within the range of our measurements. On the other hand, the differences in the concentrations of aerosols of radii around 1 μm during the storm in comparison to both the post Sharav conditions and to PG's data are obvious; our distributions have large variations in the peak at 1 μm. For comparison we plotted the size distribution which was measured during dust storm conditions at Camp Derj, Northern Sahara by Schutz and Jaenicke (1974) as well as their mean size distributions. These distributions have smaller slopes than the ones we observed during the peak and after the passage of the dust storm. In fact, their slopes more closely resemble the slope of an average size spectrum taken during a winter day in the Negev desert. On the other hand, the number concentrations of the 1 μm particles measured during the dust storm in the Sahara agree with our measurements during the period of maximum aerosol loading. The differences between the distributions probably stem from the differences in the wind

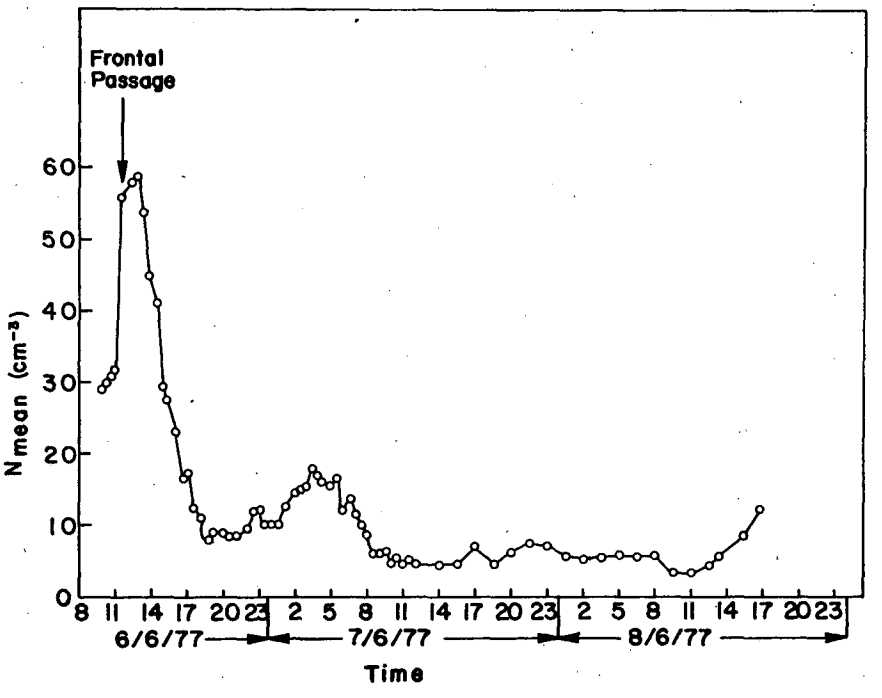

FIG. 3. Time variations of the total number concentration in the size range 0.15–12.5 μm.

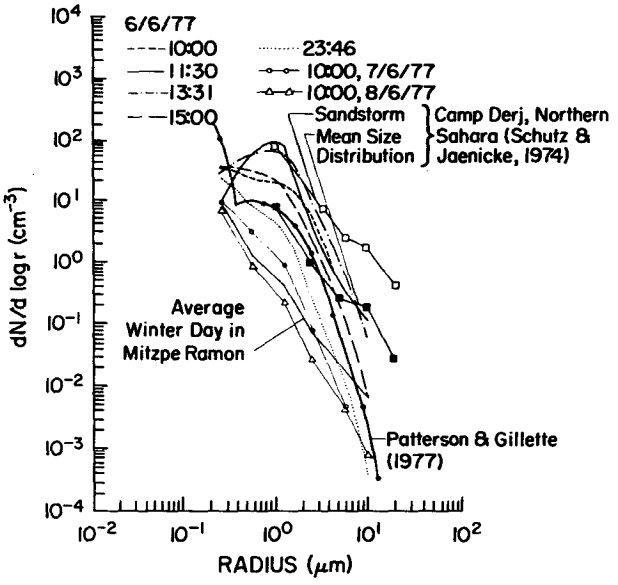

FIG. 4. Size distribution dN/d log$r$ of desert aerosol measured at surface level at Mitzpe Ramon, 6–8 June 1977 with a Royco 220.

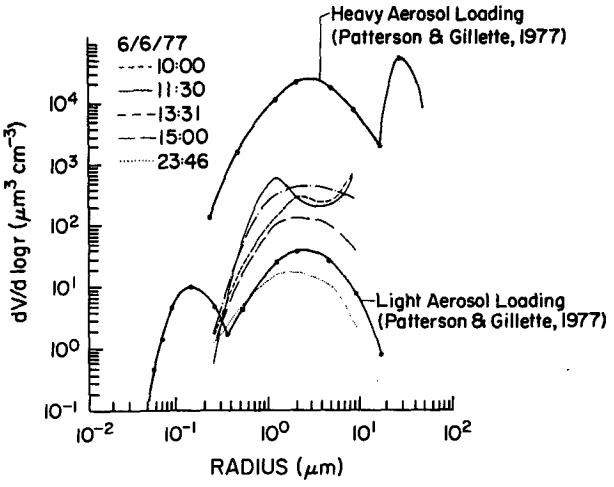

FIG. 5. Volume distributions dV/d log$r$ under conditions of Fig. 4.

speeds and hence in the intensities of the dust storms and in the composition and structure of the soils. When some of the data from Fig. 4 are plotted as volume distributions, we observe in Fig. 5 the appearance of a double mode. In addition, PG's typical volume distributions of heavy and light desert aerosol loadings are presented. Our post-Sharav distributions fall within their two, somewhat extreme, values. The shapes of most of our curves, except those at 1000 and 1130, around the passage of the cold front, agree with the general shape of the PG distributions between 0.3 and 10 μm radius. The measurements at 1000 and 1130 (during conditions of heavier aerosol loading) have a double mode distribution; both modes are located at somewhat smaller radii than those presented by PG for heavy atmospheric loading. The peak in the radius range between 1 and 10 μm is thought to be characteristic of soil-derived aerosols under all weather conditions. On the other hand, the second peak at larger radii appears only under higher wind speed conditions when local dust is generated and may therefore be related to the characteristic size spectra of the local parent soil. It is correlated with the strong decrease of horizontal visibility observed during that period (see Section 1 and Section 3c).

Fig. 6 presents the area distributions at various times in comparison with the area distributions obtained by PG for moderate aerosol loading in Plains, Texas. If one uses the PG definitions, one sees that our Sharav can be classified as an event of moderate aerosol loading. However, one should clearly note that the peaks of all our area distributions during the passage of the storm are lower than that of PG. Also, the appearance of the second mode around 1130 LST shows up at considerably smaller sizes than those shown by them.

The general conclusions that can be drawn from these measurements are as follows:

1) The Sharav produced moderate aerosol loading when compared to the scale suggested by PG, although the optical depth was very large in our case.

2) Just prior to and during the passage of the front, a sharp increase in the aerosol content is observed.

3) The shape of the size distribution is similar to that reported by other investigators, mainly for measurements taken a few hours after the front had passed.

4) Just prior to and during the passage of the front, the size distribution developed a double mode. This development is a result of locally generated dust and

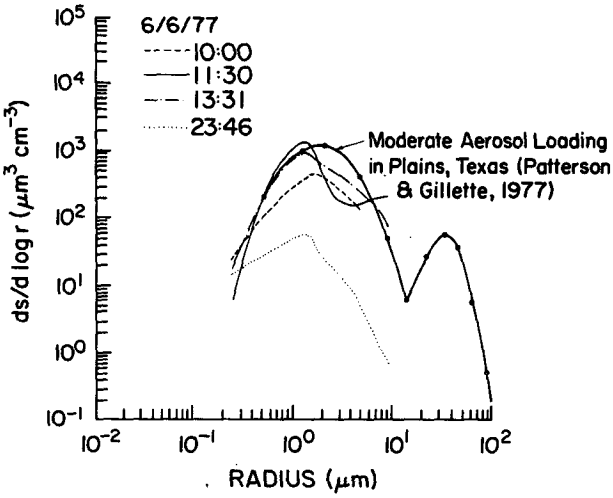

FIG. 6. Area distributions dS/d log$r$ under conditions of Fig. 4.

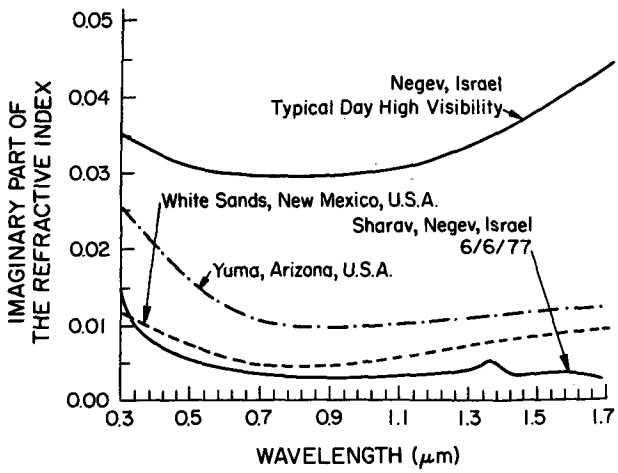

FIG. 7. The imaginary part of the refractive index in the solar spectral range during the period of the storm.

causes the peak of the size spectra to shift to larger radii (Chepil and Woodruff, 1963).

5) The general shapes of the volume and area distributions also show that the aerosol loading produced by the Sharav was moderate in intensity on the PG scale.

6) The commonality of the size distributions found by PG for soil-derived aerosols are upheld by our measurements primarily for post Sharav conditions. However, different distributions from those of PG appear at times around the passage of the cold front.

b. Imaginary refractive index

Fig. 7 represents the imaginary refractive index in the visible as measured by the reflection technique (Lindberg, 1975). As can be seen the values of this parameter during Sharav are considerably lower than those observed at the same site under clear conditions (Levin and Lindberg, 1979); however, they are fairly similar to those observed at White Sands. These differences are significant since the estimated error in the measurements by the reflection method are ~20–30% which are much lower than the differences observed under the two weather conditions. This suggests that the higher values observed in the Negev desert under clear conditions stem from the fact that the aerosols are composed of desert-type particles together with a small fraction of highly absorbing urban aerosols. Under clear conditions our Negev site is affected by winds from the north and northwest during the course of each day. The air coming from these directions carries pollutants from coastal and inland cities which absorb equally in all wavelengths in the visible range. This causes the curve of the imaginary refractive index to change its value but not its slope. On the other hand, during the Sharav itself, desert aerosols dominate. These, being particles of low absorption, cause a drastic reduction in the imaginary refractive index. The similarity between the absorptivities in the visible range during Sharav conditions and those measured at White Sands suggest that pure desert aerosols have very low absorption (in the visible) regardless of their sources. This commonality in the imaginary refractive index is very important for evaluations of global or regional effects of desert aerosols.

It should be pointed out that some commonality is also observed in the thermal IR absorption spectra. All desert aerosols show strong absorption peaks in the 8–12 μm atmospheric transparency window (e.g., Volz, 1973; Fischer, 1976; Levin, and Lindberg, 1979). The variations in the wavelengths of the absorption peaks stem from the temporal and spatial variations in the chemical composition of the particles at the various sites of observation.

c. Spectral transmission of the atmosphere

The aerosol optical depth $\tau_D(\lambda)$ at each wavelength is calculated from the averaged measurements by using

$$\tau_D(\lambda) = \left[\ln \frac{I(\lambda)}{I_0(\lambda)} - \tau_R(\lambda) \frac{P}{P_0} - \tau_{O_3}(\lambda) \right] \sec\theta_0,$$

where

$I(\lambda)$ measurement of solar direct flux at wavelength λ

$I_0(\lambda)$ measurement at top of atmosphere (from each day's calibrations, that of the previous day or from an absolute calibration)

$\tau_R(\lambda)$ Rayleigh optical depth at wavelength λ

P/P_0 pressure in units of standard pressure

$\tau_{O_3}(\lambda)$ ozone optical depth; climatological averages are used, because aerosol optical depths are larger than all others by a large factor.

We assume that atmospheric forward scattering effects in the field of view are negligible (e.g., Grassl, 1970) and that we may use $\sec\theta_0$ for the effective air mass at all measurement times (valid for $\mu_0 > 0.25$) and for all scatterers and absorbers (strictly valid if all are well mixed). The actual value of the air mass $\sec\theta_0$ is calculated from the average time of the measurement and the location of the station.

The values of $\tau(\lambda)$ for $\lambda = 0.45, 0.55, 0.65, 0.85$ and 1.0 μm are prepared in two ways for further analysis. First, we calculate $R(\lambda) = \tau(\lambda)/\tau(0.45)$ to make the data independent of total amount. This ratio is then fitted to $A(\lambda/0.45)^{-\alpha}$ by the method of least squares. This is done to facilitate comparison to the large volume of data available in the literature, derived both empirically and theoretically, in the form $\tau = \beta_0\lambda^{-\alpha}$, where $\alpha \geq 0$ in many cases

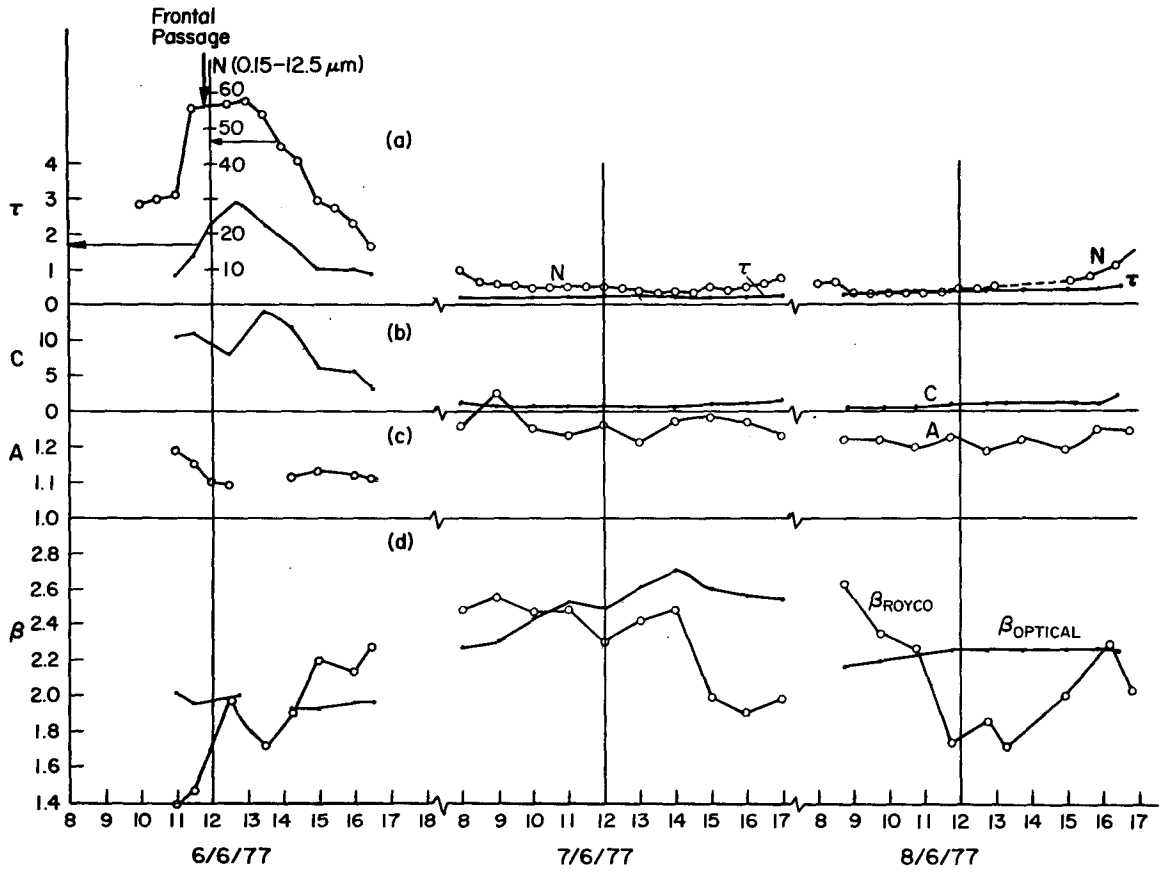

FIG. 8. The total mean number-density N (as in Fig. 3) and the optical depth τ_1 at wavelength 0.45 μm (a); the constant C of the average power-law size distribution [Eq. (1)] (b); the constant A of the average wavelength dependence of the optical depth [$\tau(\lambda) = \tau_1 A(\lambda/0.45)^{-\alpha}$] (c); and the average slope of the size distribution β derived from *in situ* (Royco) and optical data (d).

(Angstrom, 1929, 1961; Junge, 1963; Deirmendjian, 1969; etc.) but may also be negative.

We added the factor A to indicate the possible departure ($A \neq 1$) of the optical depth from that for a simple power-law size distribution. Such departures occur especially in the size range $0.1 \leq r < 2$ μm to which the optical measurements are most sensitive (e.g., Junge, 1972; Schutz and Jaenicke, 1974; Twitty *et al.*, 1976; De Luisi *et al.*, 1976a,b). In order to compare the optical with the Royco data, the latter were averaged into a power law form

$$\frac{dN}{d\ \log r} = Cr^{-\beta_{\text{Royco}}}. \qquad (1)$$

Some of the data are summarized in Fig. 8 and in Table 1. Fig. 9a shows the variation of two optical depths at two wavelengths, $\tau(0.45)$ and $\tau(0.65)$, with time on the day of the Sharav (Khamsin), 6 June 1977, and for two days afterward. All optical depths increased to values larger than 3 during the dust storm, almost independently of wavelength. The relative independence of the optical depth of wavelength is also shown in Fig. 9b and Table 1; α is close to zero during the storm. After the storm, the optical depths were only weakly dependent on wavelength on 7 June and again almost neutral on 8 June when a weak dust storm developed (see also Table 1 and Fig. 8).

The optical depth during the two days following the storm was almost an order of magnitude smaller, although still higher than normal for the time of year (Joseph and Manes, 1971; Joseph *et al.*, 1973).

The parameter A was significantly different from 1 (see Fig. 8 and Table 1), showing that the size distribution was different from a simple power law. The power α (Fig. 9b and Table 1) of the average wavelength dependence was close to zero and negative on 6 June, showing that the particles were large. These results are corroborated by the Royco measurements. On the two days following the storm, α climbed to 0.2–0.5, which is still much lower than normal (Joseph *et al.*, 1973).

Returning to Fig. 8, we may compare a and b. It is

TABLE 1. Properties of aerosols on 6–8 June 1977.

Date	Time	$*\mu_0^{-1}$	$\tau_{(0.45)}$	$**A$	$**\alpha$	β_{optical}	β_{Royco}	C_{Royco}
		a. Fit to power-law size distribution $dN/d\log r = Cr^{-\beta}$						
6 June 77	1100	1.037	0.84	1.19	0.05	2.05	1.38	10.60
	1130	1.016	1.33	1.15	−0.04	1.96	1.46	10.13
	1200	1.009	2.30	1.10	−0.04	1.96	—	—
	1230	—	—	—	—	—	1.97	7.93
	1245	1.025	2.87	1.09	0.003	2.00	1.84	—
	1330	1.075	2.22	—	—	—	1.71	13.80
	1415	1.168	1.69	1.11	−0.08	2.92	1.89	11.77
	1505	1.342	1.02	1.13	−0.08	1.92	2.19	5.91
	1550	1.606	1.00	1.12	−0.04	1.96	2.13	5.54
	1630	2.00	0.90	1.11	−0.04	1.96	2.27	3.12
7 June 77	0805	1.636	0.21	1.26	0.27	2.27	2.48	0.85
	0900	1.316	0.21	1.35	0.30	2.30	2.55	0.53
	1000	1.129	0.23	1.25	0.43	2.43	2.46	0.53
	1100	1.037	0.20	1.23	0.52	2.52	2.48	0.52
	1200	1.009	0.24	1.26	0.49	2.49	2.30	0.56
	1255	1.033	0.25	1.21	0.61	2.61	2.42	0.37
	1405	1.142	0.22	1.27	0.70	2.70	2.48	0.37
	1500	1.319	0.22	1.28	0.60	2.60	1.99	0.77
	1600	1.683	0.22	1.27	0.56	2.56	1.90	0.85
	1700	2.479	0.25	1.23	0.54	2.54	1.98	1.56
8 June 77	0845	1.385	0.29	1.22	0.17	2.17	2.63	0.35
	0945	1.165	0.33	1.22	0.20	2.20	2.35	0.33
	1045	1.053	0.36	1.20	0.23	2.23	2.27	0.36
	1145	1.010	0.36	1.23	0.27	2.27	1.74	0.74
	1245	1.025	0.40	1.19	0.32	2.32	1.86	0.82
	1345	1.100	0.38	1.22	0.29	2.29	1.71	1.03
	1503	1.339	0.41	1.19	0.33	2.33	2.00	1.07
	1545	1.565	0.35	1.25	0.33	2.33	2.30	1.01
	1630	1.991	0.36	1.23	0.24	2.24	2.03	2.17
	1700	2.471	0.37	1.20	0.27	2.27	—	—

Time	$\tau_{(0.45\ \mu m)}$	$\tau_{(0.55\ \mu m)}$	$\tau_{(0.65\ \mu m)}$	$\tau_{(0.84\ \mu m)}$	$\tau_{(1.04\ \mu m)}$
	b. The optical depth of dust on 6 June 1977				
1100	0.84	1.05	1.30	0.94	0.93
1130	1.33	1.62	1.93	1.53	1.53
1200	2.30	2.60	2.99	2.58	2.58
1245	2.87	3.17	3.56	3.09	3.06
1330	2.22	—	2.89	2.50	2.62
1415	1.69	1.97	2.29	1.89	2.01
1505	1.02	1.23	1.46	1.16	1.23
1550	1.00	1.16	1.38	1.09	1.15
1630	0.90	1.04	1.22	0.97	1.03

* μ_0^{-1} = (cosine solar zenith angle)$^{-1}$.

** $\dfrac{\tau(\lambda)}{\tau(\lambda_1)} = A\left(\dfrac{\lambda}{\lambda_1}\right)^{-\alpha}$.

clear that the optical depth τ is highly correlated to the total number of particles N as well as to the constant C of the power-law distribution fitted to the Royco data. The general shape of the curves is similar, although the details in the Royco data are not present in the optical depth.

The latter fact is even clearer from both Fig. 8 and Table 1 where we compared β_{Royco} and β_{optical}. The value of β_{optical} was calculated from the exponent of the wavelength dependence of the optical depth α (see Table 1) and is equal to $\beta_{\text{optical}} = 2 + \alpha$.

The average level of β_{optical} follows that of β_{Royco} on all three days, including 8 June when there occurred a weak dust storm. On the other hand, the optical method is unable to follow the fluctuations in β_{Royco} especially for large optical depth (6 June) or during the occurrence of dust increases (8 June). This is for several reasons. First, the optical measurement integrates over the whole atmosphere,

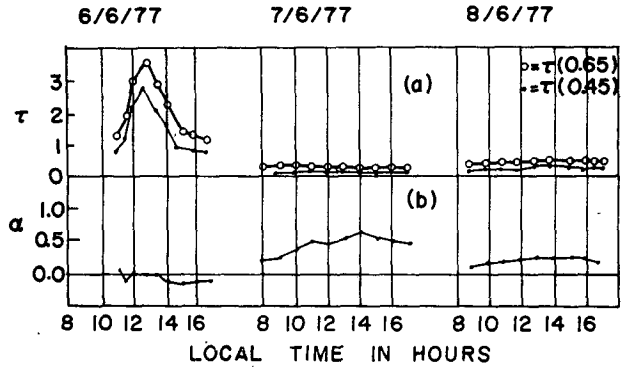

FIG. 9. Time variations of the optical depths $\tau(0.45\ \mu m)$ and $\tau(0.65\ \mu m)$ and the wavelength exponent α.

whereas the Royco data are for surface conditions only, where larger particles are more prevalent and fluctuation in the latter's amount more dominant. Second, the optical measurement integrates over all sizes between 0.1 and 1.0 to 2 μm. Third, much of the fluctuations are in the large particle fraction ($r > 1\ \mu m$) to which the optical method is relatively insensitive.

In Fig. 10 we compare some typical optical depths during the presently described dust storm with the average Sharav optical depths for the years 1971–72—a ratio of 3:1 is seen to occur—and with the average optical depths during cloud-free days in the years 1971–73—a ratio of 10:1 and larger occurs.

Furthermore, we compare with average and high optical depths of the Saharan aerosol layer over the Atlantic Ocean in summer (Carlson and Caverly, 1977), and with values for a cloud-free summer day, 13 September 1977, in the high Negev Desert. In all cases, the high optical depths occurring during the dust storm described in this paper are clearly brought out.

Such optical depths as observed during the dust storm usually occur for less than 10% of the year. However, slightly smaller optical depths of the order of 1, are found to be common over the low altitude Atlantic ocean (Carlson and Caverly, 1977) as well as over the Middle East.

The whole range of optical depths we have just described is at least an order of magnitude larger than that of the Rayleigh atmosphere at the same wavelengths (0.36–1.01 μm). Similarly, the dust

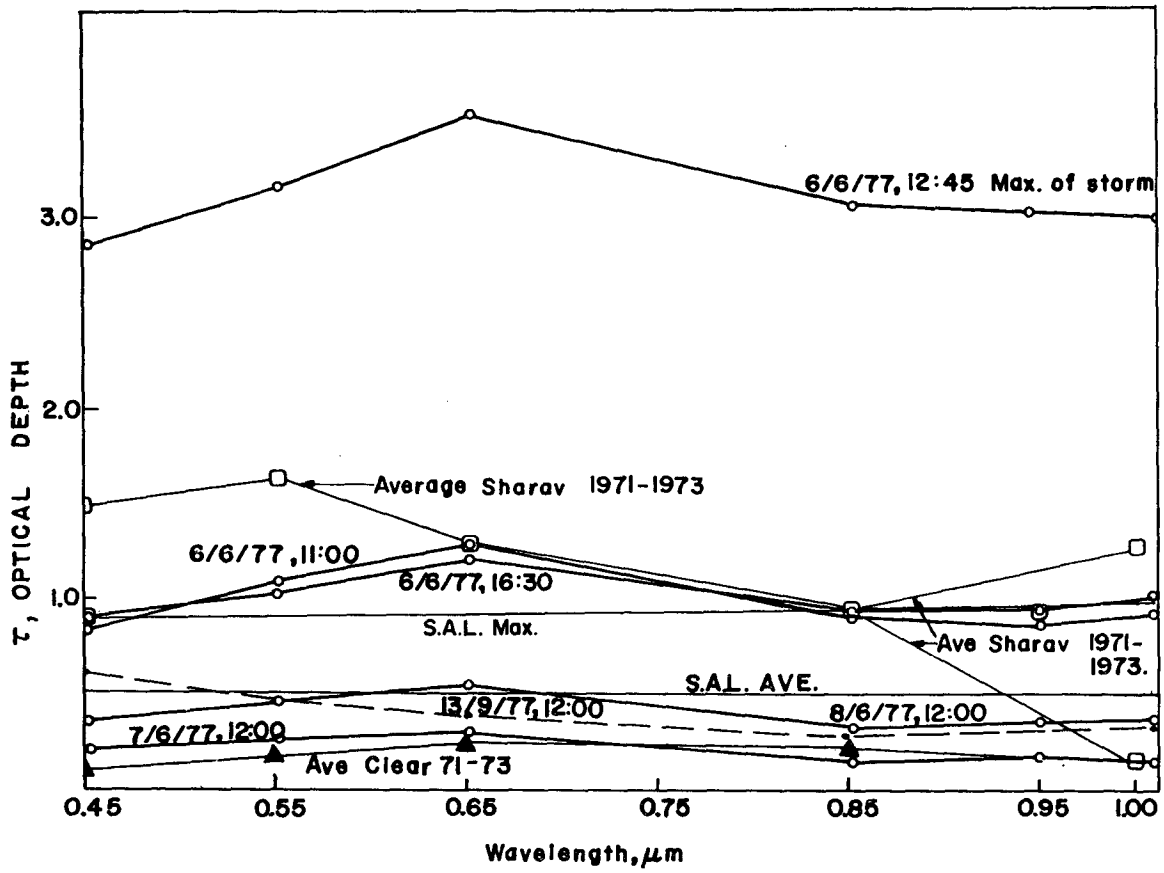

FIG. 10. Typical curves of optical depth versus wavelength during the storm compared to data from other locations and from other times at Mitzpe Ramon (SAL stands for Saharan Aerosol Layer).

optical depths during the Sharav are much larger than those of either water vapor or ozone in their absorption bands in the solar spectrum. The suitability of this storm for isolating the properties of the regional desert dust aerosol is thus obvious.

4. Summary and conclusions

The present study compares the properties of desert aerosol in the Middle East as measured by direct sampling and by spectral transmission of solar radiation. Such comparisons are of importance due to the need to extract as much information as possible from large-scale remote sensing of aerosols in order to describe the latter's spatial and temporal variations for use in climate related studies as well as in the determination of long-range slant visibility and of sea surface temperature from satellite data. The measured aerosol size distribution after the passage of the front was found to be similar to distributions measured by other investigators at other desert sites. This points to some commonality (Patterson and Gillette, 1977) in desert aerosols around the world.

We have shown that the general time trends of the size distribution as measured *in situ* are followed by the optical depth and its variation with wavelength. This may mean that the aerosol is often quite well mixed. On the other hand, detailed short-term fluctuations are not followed for the various reasons mentioned in Section 3.

We have observed that the simplest power law approximation poorly represents the size distribution of the aerosols during the peak of the dust storm. However, the fit to a power law improves as the aerosol loading approaches that of normal weather conditions. A pure power law size distribution is not usually found. During periods of low dust load, conditions are such that the average slope of the size distributions derived from optical measurements agrees with those from *in situ* Royco observations.

It follows from our discussion that it will be difficult to ascertain the exact size distributions from remote optical observations at any given location. On the other hand, it also means that it is probably not important to resolve the exact size distribution with high resolution as to size and variability, at a given time in order to estimate the effects of an aerosol on the atmospheric energy balance. All aerosol size distributions with the same total number of particles, mean size and mean width will probably have the same optical effects (e.g., Hansen and Travis, 1974). The imaginary part of the refractive index during the Sharav (Khamsin) period is lower by a factor of 3–5 than that during normal weather and quite similar to the values found in the U.S. Southwest and over the Atlantic Ocean. This shows again that desert aerosol is a distinct global type. Second, it shows that during normal weather situations, the contribution of the highly absorbing urban or organic aerosol to the imaginary part of the refractive index is important. Desert aerosol being composed primarily of silicaceous clays, shows strong absorption bands in the 8–12 μm atmospheric window (e.g., Fischer, 1976; Levin and Lindberg, 1979; Grassl, 1973; Volz, 1973). The radiative effects of the desert aerosol are thus sensitively balanced between two opposing effects—the increase of earth–atmosphere albedo and the partition of absorbed solar radiation between surface and atmosphere in the solar spectral range—leading to heating of the affected layers and cooling of the underlying surface and the increase of the greenhouse effect in the thermal IR due to clogging of the 8–12 μm window.

Acknowledgments. We would like to thank Mr. Baruch Starobinets and Mr. N. Sandlerman for their excellent aid in building and maintaining the equipment.

One part of this study was financed by the Israel-U.S. Bi-National Science Foundation under Grant 304.

Other parts of this work were carried out under the sponsorship of the U.S. Army, ERO, under Grant DAERO-78-G-087.

REFERENCES

Angstrom, A., 1929: On the atmospheric transmission of sun radiation and on dust in the air. *Geogr. Ann.*, **11**, 156.

——, 1961: Techniques of determining the turbidity of the atmosphere. *Tellus*, **13**, 214–223.

Carlson, T. N., 1976: Large-scale distribution of turbidity over the Northern Equatorial Atlantic. *Proceedings of the Symposium on Radiation in the Atmosphere*, H. J. Bolle, Ed., Science Press, 555–556.

——, J. M. Prospero, 1972: Vertical and real distribution of Saharan dust over the western equatorial North Atlantic Ocean. *J. Geophys. Res.*, **77**, 5255–5265.

——, and R. S. Caverly, 1977: Radiative characteristics of Saharan dust at solar wavelengths. *J. Geophys. Res.*, **82**, 3141–3152.

Chepil, W. S., and N. P. Woodruff, 1963: The physics of wind erosion and its control. *Advances in Agronomy*, Vol. 15, Academic Press, 211–302.

Deirmendjian, D., 1969: *Electromagnetic Scattering on Spherical Poly-Dispersions*. Elsevier Press, 290 pp.

DeLuisi, J. J., P. M. Furukawa, D. A. Gillette, B. G. Schuster, R. J. Charlson, W. M. Porch, R. W. Fegley, B. M. Herman, R. A. Rabinoff, J. T. Twitty and J. A. Weinman, 1976a: Results of a comprehensive atmospheric aerosol-radiation experiment in the southwestern United States: Part I. Size distribution, extinction, optical depth and vertical profiles of aerosols suspended in the atmosphere. *J. Appl. Meteor.*, **15**, 441–454.

——, ——, ——, ——, ——, ——, ——, ——, ——, ——, ——, ——, and ——, 1976b: Results of a comprehensive atmospheric aerosol-radiation experiment in the southwestern United States: Part II. Radiation flux measurements and theoretical interpretation. *J. Appl. Meteor.*, **15**, 455–463.

Fischer, K., 1976: The optical constants of atmospheric aerosol

particles in the 7.5–1.2 μm spectral region. *Tellus*, **28**, 266–274.

Goldberg, E. D., 1971: Atmospheric dust—the sedimentary cycle and man. Comments on Earth Sciences. *Geophysica*, **1**, 117–132.

Grassl, H., 1970: Determination of cloud drop size distribution from spectral transmission measurements. *Contrib. Atmos. Phys.*, **43**, 255–284.

——, 1973: Separation of atmospheric absorbers in the 8–13 μm region. *Contrib. Atmos. Phys.*, **46**, 75–88.

Hansen, J. E., and L. T. Travis, 1974: Light scattering in planetary atmospheres. *Space Sci. Rev.*, **16**, 527–610.

Joseph, J. H., 1976: The effect of a desert aerosol on a model of the general circulation. *Proceedings of the Symposium Radiation in the Atmosphere*, H. J. Bolle, Ed., Science Press, 487–492.

——, and A. Manes, 1971: Secular and seasonal variations of the atmospheric turbidity in Israel at Jerusalem. *J. Appl. Meteor.*, **10**, 453–462.

——, and N. Wolfson, 1975: The ratio of absorption to backscatter of solar radiation during Khamsin conditions and effects on the radiation balance. *J. Appl. Meteor.*, **14**, 1389–1396.

——, A. Manes and D. Ashbel, 1973: Desert aerosols transported by Khamsinic depressions and their climatic effects. *J. Appl. Meteor.*, **12**, 792–797.

Junge, C., 1963: *Air Chemistry and Radioactivity*. Academic Press, 382 pp.

——, 1972: Our knowledge of physico-chemistry of aerosols in the undisturbed environment. *J. Geophys. Res.*, **77**, 5183–5200.

King, M. D., D. M. Byrne, B. M. Herman and J. A. Reagan, 1978: Aerosol size distributions obtained by inversion of spectral optical depth measurements. *J. Atmos. Sci.*, **35**, 2153–2167.

Levin, Z., and J. Lindberg, 1979: Size distribution, chemical composition and optical properties of urban and desert aerosols in Israel. *J. Geophys. Res.*, **84**, 6941–6950.

Lindberg, J. D., 1975: The composition and optical absorption coefficient of atmospheric particulate matter. *Opt. Quant. Electron.*, **7**, 131–139.

Patterson, E. M., and D. A. Gillette, 1977: Commonalities in measured size distributions for aerosols having a soil derived component. *J. Geophys. Res.*, **82**, 2074–2082.

Schutz, L., and R. Jaenicke, 1974: Particle number and mass distributions above 10^{-4} cm radius in sand and aerosol of the Sahara Desert. *J. Appl. Meteor.*, **13**, 863–870.

Shipley, S., J. H. Joseph, J. T. Trauger, P. J. Guetter, E. W. Eloranta, J. E. Lawler, W. J. Wiscombe, A. P. Odell, F. L. Roester and J. A. Weinman, 1975: The evaluation of a shuttle-borne lidar experiment to measure the global distribution of aerosols and their effect on the atmospheric heat budget. Final Report, NASA Grant NSG 1057, 150 pp.

SMIC, 1971: Inadvertent Climate Modification Report. *Study of Man's Impact on Climate*, The MIT Press, 308 pp.

Twitty, J. T., R. J. Parent, J. A. Weinman and E. W. Eloranta, 1976: Aerosol size-distributions: remote determination from airborne measurements of the solar aureole. *Appl. Opt.*, **15**, 980–989.

Volz, F. E., 1973: Infra-red constants of ammonium sulfate, Sahara dust, volcanic pumice and flyash. *Appl. Opt.*, **12**, 564–568.